

Solar Radio Noise Storms Observed at Coho Radio Observatory in September 2017

Whitham D. Reeve

1. Introduction

The autumn of 2017 saw considerable solar activity despite being near the end of the current solar cycle. When activity occurs in the low part of the cycle it often is quite intense as was the case in September and October. This activity included many intense flares and radio bursts. In this paper I report on Type I solar radio noise storms observed in circular polarization on 7 and 26 September. I previously reported on a Type II slow sweep radio burst and associated coronal mass ejection on 20 October [\[Reeve18-1\]](#), a radio blackout caused by an X8.2 solar flare on 10 September [\[Reeve18-2\]](#) and a geomagnetic storm on 14 October [\[Reeve17\]](#).

In the following sections I provide a general description of radio noise storms (section 2) followed by a brief description of the overall solar event that produced the observed noise storms (section 3). Finally, the observed storms are described in terms of their spectra (section 4). All times are Coordinated Universal Time (UTC) unless otherwise indicated.

2. Noise Storm Characteristics

The Type I radio noise storm is one of five general types of radio emissions generated by the Sun (figure 1). The Type I consists of a long series of short duration radio bursts often accompanied by continuum radiation (continuum radiation is any radiation that has a continuous spectrum and is not limited to a narrow frequency range). During periods of intense activity hundreds of bursts may occur every hour and storms may last for days. Surrounding sunspot maximum, Type I bursting is present about 10% of the time below 200 MHz, but as the solar cycle approaches minimum, the occurrence of Type I radio noise storms decreases. Other names that often are used for Type I are *radiation storm* and *CTM* (continuum).

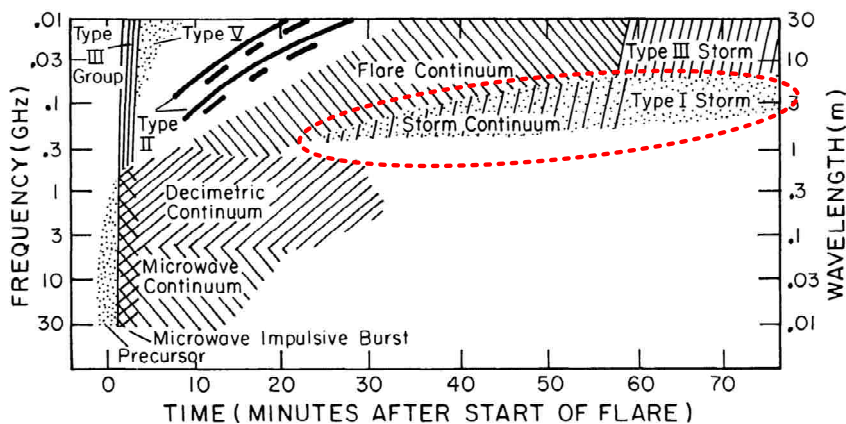


Figure 1 ~ Dynamic spectrum of solar radio bursts that might be produced by a strong flare. Burst types have been categorized as Types I through V. Individual solar events will vary greatly – some radio burst types may be weak or missing. Storm Continuum and Type I Storm, or radio noise storm, the subject of this paper, is outlined with a dotted red line. Source: Figure 11 in [Dulk]

The theoretical aspects of solar noise storms have been very difficult to develop, even after more than 70 years of observation. Like some other solar radio phenomena, the emission mechanisms of radio noise storms still are not known with certainty. However, it is known that noise storms originate from persistent sources of energetic

particles in the Sun's corona and are different in that respect from transient phenomena such as flares and Type II and III radio bursts. Many papers and at least one entire book have been written about noise storms [Elgarøy77]. From these, one can obtain the general characteristics (table 1). The emission frequencies of radio noise storms correspond to plasma frequencies at solar altitudes in the lower corona (figure 2).

Table 1 ~ Type I solar radio noise storm general characteristics.
Data from [Elgarøy77], [Sundaram04], [Mercier14]

Parameter	Description
Association with flares	Noise storms are statistically associated with flares, usually occurring within 1 h after the optical flare
Cone of emission	Narrow, strongest signal received when the source is aligned with the Sun's central meridian
Exciting agency	Thought to be magnetic reconnection associated with energetic particles trapped in a closed magnetic structure over an active region or weak shocks associated with newly emerging magnetic flux
Emission process	Thought to occur at the fundamental plasma frequency due to suprathermal (velocity much greater than the characteristic local thermal velocity) electrons trapped in closed magnetic flux tubes
Spectrum	30 to 500 MHz, but usually between 50 and 250 MHz
Continuum	May be superposition of many smaller bursts or distinct but related phenomenon
Continuum bandwidth, df/f	~100%
Continuum duration	Hours to days
Continuum intensity variability	Slow
Continuum drift	Either way at rates between Type II and Type III rates
Burst bandwidth, df/f	~3%
Individual burst duration	0.1 to 10 s
Burst shape	Steep rise and exponential decline
Polarization	Strong circular polarization (approaching 100%); continuum usually the same polarization as the bursts
Height of source	1.2 to 2.0 solar radii (R_{Sun})
Brightness temperature	500 million K at 43 MHz, 9 billion K at 169 MHz

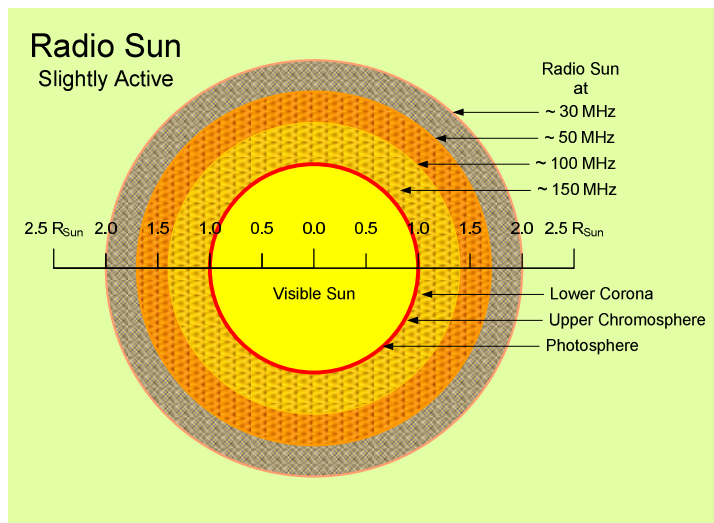


Figure 2 ~ Conceptual radio Sun, showing the distances from the center of the Sun in multiples of the visible Sun radius R_{Sun} for the characteristic plasma frequencies indicated by concentric shells. The photosphere, chromosphere and lower corona regions are indicated by callouts. The frequencies shown are based on the Newkirk corona density model for slightly active Sun. The heliocentric distance for a given frequency varies with the solar cycle and related activity, and the actual radio Sun is wider at the equator than at the poles.

3. Overall Solar Events of 7 and 26 September

The events relevant to this paper were described in daily reports issued by NOAA’s Space Weather Prediction Center (SWPC). The *Solar and Geophysical Event Report* for the days in question include the radio noise storm (RNS), continuum (CTM) and other components, such as an x-ray flare and radio bursts at various frequencies (table 2). Spacecraft imagery also is available for the Sun in various wavelengths. The Solar Dynamics Observatory (SDO) data (figure 3) does not indicate any obvious activity in x-ray wavelengths at the time of the noise storms except an active region that could be associated with the storm on 7 September.

Table 2.a ~ Extract from SWPC solar Events report from 7 September 2017 showing only the time period of the events leading up to and including the radio noise storm on that date. The radio noise storm was likely associated with the C4.5 flare at active region 2673. Source: [EVENT26](#)

#Event	Begin	Max	End	Obs	Q	Type	Loc/Frq	Particulars	Reg#
7840 +	1840	1844	1849	G15	5	XRA	1-8A	C4.5 1.8E-03	2673
7840	1841	1841	1841	SAG	G	RBR	1415	410	
7840	1841	1841	1841	SAG	G	RBR	8800	130	
7840	1841	1841	1841	SAG	G	RBR	15400	100	
....									
7720	1849	1903	2014	SAG	G	RNS	410	330	

Table 2.b ~ Extract from SWPC solar Events report from late 25 and early 26 September 2017 showing only the time period of the radio noise storm on that date. No flare was reported within 3 h of the radio noise storm but active region 2681 was close to the central meridian at the time. Data sources: [EVENT25](#), [EVENT26](#)

#Event	Begin	Max	End	Obs	Q	Type	Loc/Frq	Particulars	Reg#
25 Sep 2017									
130	2226	////	2359	LEA	C	RSP	025-180	CTM/2	
26 Sep 2017									
200	0000	0027	0114	PAL	G	RNS	245	340	
...									
140	0000	////	0735	LEA	C	RSP	025-180	CTM/2	

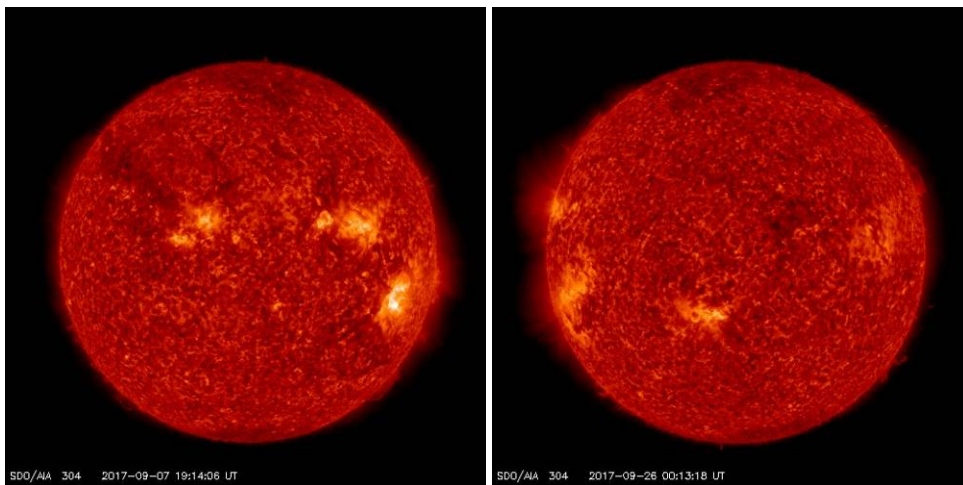


Figure 3 ~Images of the Sun at 304 Å wavelength taken at 1914 UTC on 7 September (left) and 0013 on 26 September (right) by the Solar Dynamics Observatory (SDO), at the times of the radio noise storms. In the left image, the bright region just below the 3:00 position closest to the limb is AR2673 and in the right image the bright region near the meridian is AR2681. Images source: NASA/SDO

4. Radio Observations for 7 and 26 September

The radio noise storms were observed at Cohoe Radio Observatory in Alaska (table 3 and figure 4) on 7 September between approximately 1830 and 2300 UTC and on 26 September between 0000 and 0230 UTC, both in the frequency range 45 to 93 MHz. Similar observations of the 7 September noise storm were made at the Greenland Callisto/LWA antenna station near Kangerlussuaq but not of the 26 September storm (the latter storm occurred after sunset at the Greenland station).

Table 3 ~ Callisto station details for Cohoe Radio Observatory, Alaska
Note: LWA: Long Wavelength Array, AMSL: Above Mean Sea Level

Parameter	Value
Geographical coordinates	60° 22' 4.7" N, 151° 18' 54.5" W
Elevation	22 m AMSL
Frequency settings	45 to 93 MHz
Number of usable channels	192
Frequency resolution	250 kHz
Sweep rate	800 ch s ⁻¹
Instantaneous bandwidth	300 kHz
Integration time	1 ms
Antenna	LWA (active crossed-dipole)
Polarization	Right- and Left-Circular



Figure 4 ~ Cohoe Radio Observatory is located in southcentral Alaska on the Kenai Peninsula near the Kasilof River. Underlying image source: USGS

The length of the 7 September noise storm as observed at CRO (4 h 10 min) was much longer than reported by SWPC (1 h 26 min). Similarly, the length of the 26 September noise storm as observed at CRO (2 h 30 min) was longer than reported by SWPC (1 h 14 min). Also note that SWPC reported the data for the two storms at much higher frequencies than observed at CRO and this probably accounts for the different elapsed times. SWPC reported at 410 MHz for 7 September and 245 MHz for 26 September, both at the upper limits for the large majority of radio noise storms (see section 2).

For reference, solar positional data with respect to CRO is provided for each storm (table 4). The radio observations were made with an LWA antenna and LWA power coupler with quadrature coupler along with two Callisto instruments, one for each direction of circular polarization. Additional descriptions of the instrumentation are in the *Appendix*. The Callistos were setup to produce Flexible Image Transport System (FITS) data files with 15 minute lengths, nominal 200 frequency channels and four observations per second at each

frequency (sweep rate of 800 channels s⁻¹ producing 3600 x 200 pixels in each 15 min period). These files were processed to produce the spectra shown below.

Table 4 ~ Solar positions at Cohoe Radio Observatory at time of radio noise storm maximums. The elapsed times are based on SWPC x-ray flare data previously listed (not CRO radio observations)

Date (2017)	Time (UTC)	Solar elevation (°)	Solar azimuth (°)	Flare elapsed time (min)
7 September	1903	25.8	128.6	85
26 September	0027	21.9	221.1	74

Spectra: The spectra for each event in each polarization (LHCP and RHCP) are provided in this subsection. As previously mentioned, the observed storm lengths were 4 h 10 min and 2 h 30 min for 7 and 26 September, respectively. For easy comparison, the dynamic spectra plots show intervals of 15 min during the most intense part of the storms and also for durations of 2 h 30 min (figure 5).

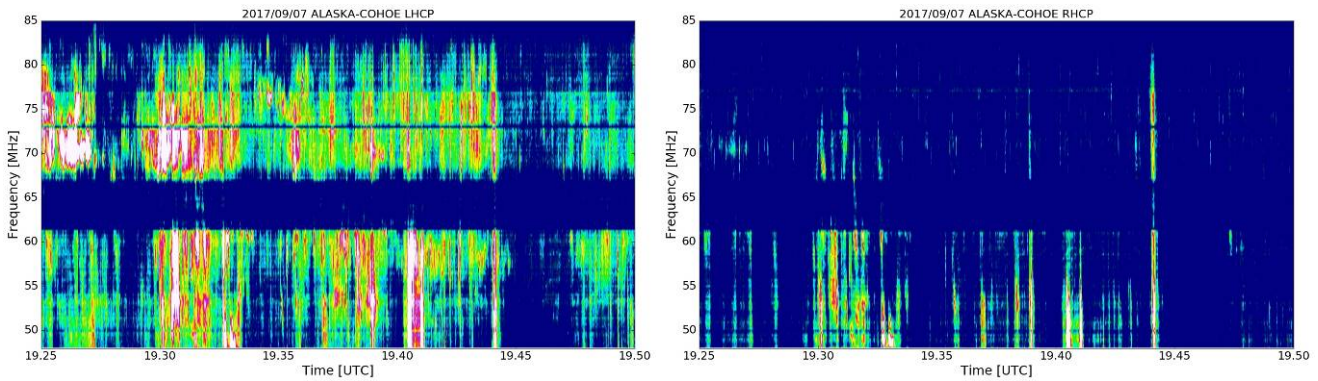


Image 5-1 (LHCP) & 5-2 (RHCP): 15 min period showing the peak time of the noise storm on 7 September. See overall caption below.

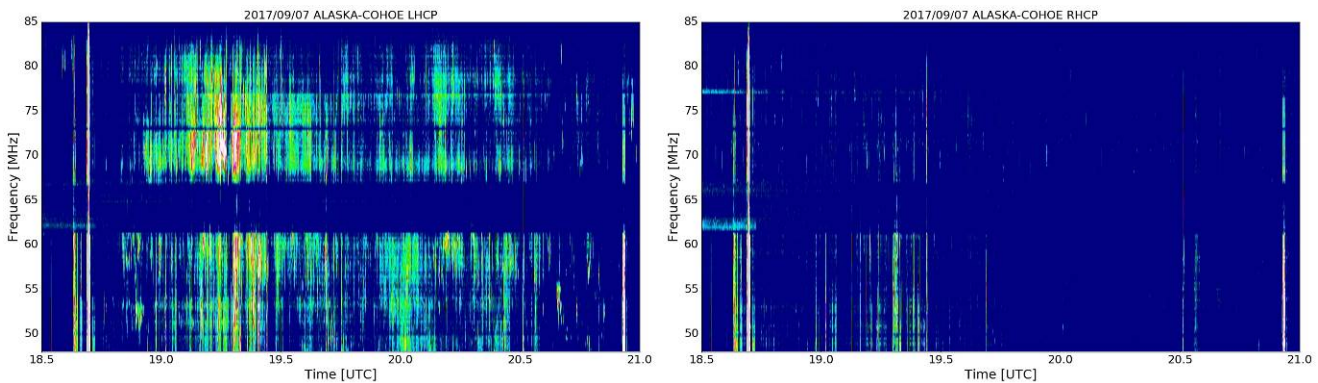


Image 5-3 (LHCP) & 5-4 (RHCP): 2 h 30 min period showing the entire observed noise storm on 7 September. See overall caption below.

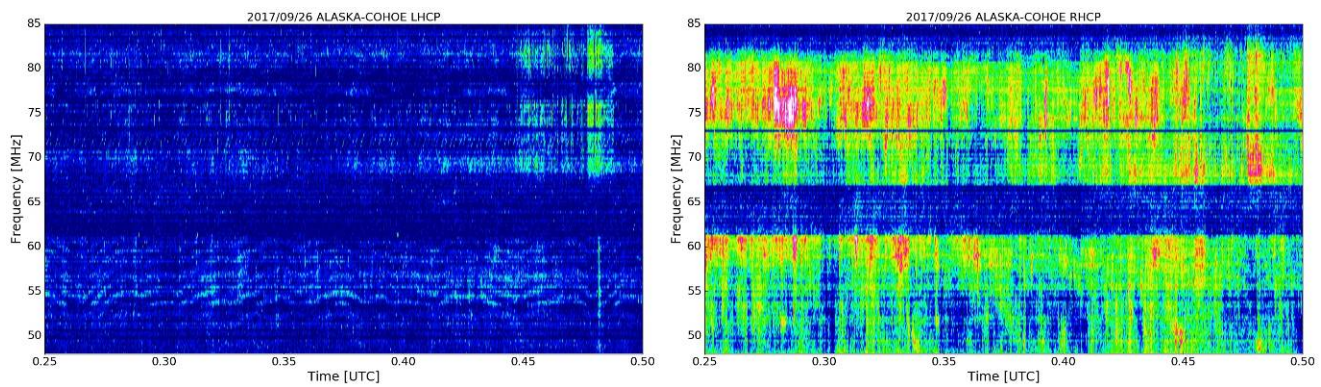


Image 5-5 (LHCP) & 5-6 (RHCP): 15 min period showing the peak of the noise storm on 26 September. See overall caption below.

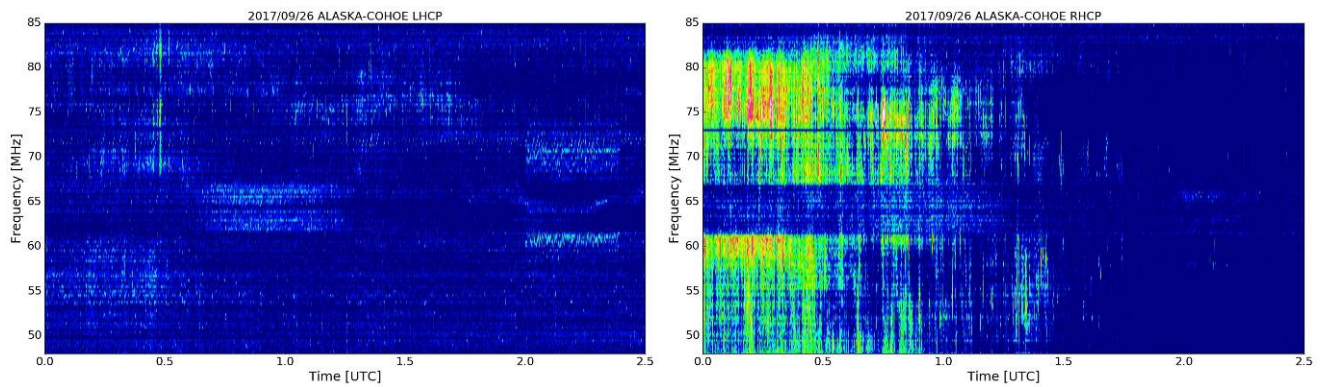


Image 5-7 (LHCP) and 5-8 (RHCP): 2 h 30 min period showing the entire observed noise storm on 26 September. See overall caption below.

Figure 5 ~ Left-hand circular and Right-hand circular polarizations (left and right images, respectively). Each pixel in the images represents a particular time, frequency and relative intensity of the received emissions. Background noise is computed for each image and subtracted. Time (UTC) is shown on the bottom horizontal scales in decimal notation. Frequency (MHz) is shown on the left vertical scale starting at 48 MHz at the bottom and increasing upward. The relative received intensity is represented by colors with low-to-high intensities shown in blue-cyan-green-yellow-red-violet-white. The very large majority of near-vertical streaks are Type I radio bursts but some Type III fast sweep radio bursts are interspersed especially in the 7 September storm. The Type III bursts appear in both polarizations. The dark band centered on 64 MHz is intermodulation from FM broadcast transmitters, which effectively blocks reception of the weak solar radio activity on those frequencies. The roll-off in response above approximately 82 MHz may be for the same reason. All plots were produced by a custom Python application (see section 7, Acknowledgements). For reference, the color map was set to “gist_ncar”, the images for 7 September used $V_{min}=2$, $V_{max}=15$ and images for 26 September used $V_{min}=0$, $V_{max}=9$.

Discussion: The radio noise storm on 7 September was primarily left-hand circular polarized (LHCP) and on 26 September was primarily right-hand circular polarized (RHCP). Interspersed in the noise storm spectra for 7 September are numerous Type III fast-sweep radio bursts. Type III radio bursts normally are unpolarized or weakly polarized and, thus, appear in spectra of both polarizations.

Note: The polarization rotation directions are based on mathematical analysis of the quadrature coupler used with the LWA antenna (see Appendix), but I have not yet obtained comparable data from a professional observatory to confirm the directions. Therefore, the rotation directions described here are subject to change.

5. Conclusions

Type I solar radio noise storms are described in this paper with emphasis on storms observed 7 and 26 September 2017 at Coho Radio Observatory in Alaska. These noise storms generally emit in the VHF band and consist of large numbers of very short radio bursts, often accompanied by a radio continuum and lasting for hours to days. Type I radio noise storms are very interesting because, in spite of 70 years of very detailed observations by professional investigators, the emission mechanisms have not been clearly identified and are not yet clearly understood.

6. References and Web Links

e-Callisto data for all stations including Coho:

Daily Quickviews of solar radio spectra: http://soleil.i4ds.ch/solarradio/data/1998-2009_quickviews/

Daily Lightcurves of solar radio data: <http://soleil.i4ds.ch/solarradio/data/Lightcurves/>

15-minute FITS data from which the spectra and lightcurves are produced as well as associated spectra images: <http://soleil.i4ds.ch/solarradio/callistoQuicklooks/>

- [Dulk] Dulk, G., Radio Emission from the Sun and Stars, Annual Reviews of Astronomy & Astrophysics, 23: 169-224, 1985. Available at: <http://adsabs.harvard.edu/abs/1985ARA%26A..23..169D>
- [Elgarøy77] Elgarøy, Ø., Solar Noise Storms, Vol. 90, International Series in Natural Philosophy, Pergamon Press, 1977
- [Kraus] Kraus, J., Radio Astronomy, 2nd Ed., Cygnus-Quasar Books, 1986
- [Marr] Marr, J., Snell, R. and Kurtz, S., Fundamentals of Radio Astronomy – Observational Methods, CRC Press, 2016
- [Sundaram04] Sundaram, G., Subramanian, K., Spectrum of Solar Type I Continuum Noise Storm in the 50-80 MHz Band and Plasma Characteristics in the Associated Source Region, The Astrophysical Journal, 605:948-959, 2004 April 20. Available at: <https://arxiv.org/abs/astro-ph/0401380>
- {Mercier] Mercier, C., Subramanian, P., Chambe, G., Janardhan, P., The Structure of Solar Radio Noise Storms, Astronomy & Astrophysics, 576, A136 (2015), DOI: 10.1051/0004-6361/201321064, ESO 2015. Available at:
- {EVENT07} <ftp://ftp.swpc.noaa.gov/pub/indices/events/20170907events.txt>
- {EVENT25} <ftp://ftp.swpc.noaa.gov/pub/indices/events/20170925events.txt>
- {EVENT26} <ftp://ftp.swpc.noaa.gov/pub/indices/events/20170926events.txt>
- {Reeve17} Reeve, W., Observations of Geomagnetic Storm Conditions at Anchorage, Alaska on 14 October 2017, 2017. Available at: http://www.reeve.com/Documents/Articles%20Papers/Observations/Reeve_Mag_CHSS_14Oct2017.pdf
- {Reeve18-1} Reeve, W., Type II Solar Radio Burst Observed on 20 October 2017, 2018. Available at: http://www.reeve.com/Documents/CALLISTO/Reeve_Typell-Burst.pdf
- {Reeve18-2} Reeve, W. Propagation Effects on WWV-15 by Solar Activity ~ Received at Anchorage, Alaska USA on 10 September 2017, 2018. Available at: http://www.reeve.com/Documents/Articles%20Papers/Reeve_15MHzSolarPropEff.pdf

7. Acknowledgements

I am once again indebted to Christian Monstein, who developed the Python code that I used to plot the Callisto FITS files.

Appendix ~Instrumentation

The instrumentation at Cohoe Radio Observatory is briefly described by an RF system block diagram (figure A-1) and a few pictures of the instrumentation (figure A-2). A dual Callisto installation is connected to a Long Wavelength Array (LWA) antenna, one instrument for each polarization. The Callisto has a native frequency range of 45 to 870 MHz and 62.5 kHz frequency resolution. The instrument's programmable frequency range is reduced to 45 to 93 MHz for compatibility with the antenna. It is setup for 192 usable channels with 250 kHz spacing as determined by a frequency configuration file in the Callisto software. When in operation, each Callisto consumes about 2.8 W at 12 Vdc.

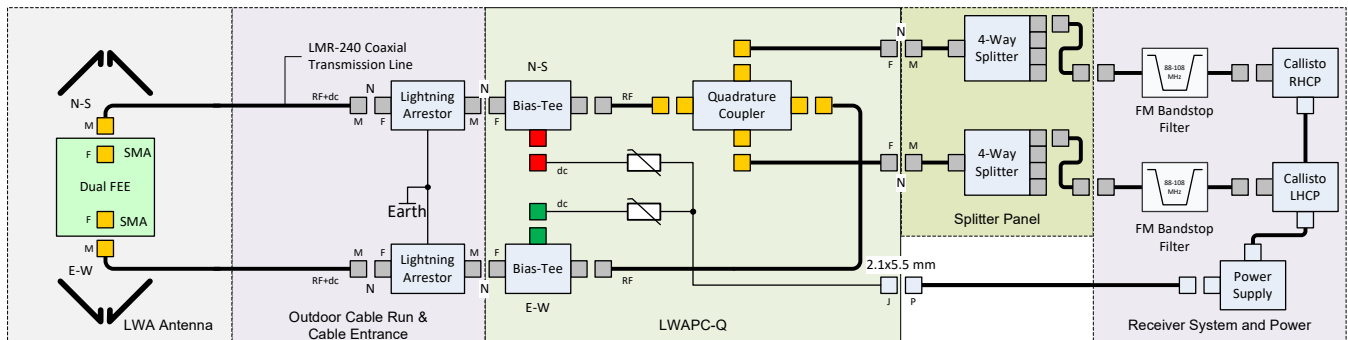


Figure A-1 ~ RF system block diagram. The major blocks are, left-to-right, the LWA antenna, coaxial cable transmission lines and cable entrance facility with lightning arrestors, LWA Power Coupler, 4-way Splitter Panel, Callisto instruments and associated power supplies.

The antenna is a sloping elements crossed-dipole with a frequency range of 5 to 100 MHz. Front-end electronics (FEE) consisting of dual low noises amplifiers (LNA) are installed at the junction of the elements, making the LWA antenna an active antenna. Each LNA in the FEE consumes approximately 3.5 W at 15 Vdc and provides 35 dB gain. The FEE noise figure is 2.9 dB and because of its high gain the FEE dominates the system noise figure. Antenna power is provided by an LWA Power Coupler with quadrature coupler (LWAPC-Q). The LWAPC-Q includes two bias-tee modules, power input filtering and overcurrent protection. The quadrature coupler provides right-hand and left-hand circular polarizations (RHCP and LHCP, respectively) from the two linearly polarized dipoles. The RHCP and LHCP outputs from the LWAPC-Q are connected to 4-way RF splitters that allow connection of multiple receivers. Unused splitter ports are resistively terminated.

The Callisto instruments are controlled by small desktop PC running Windows 10 operating system. Two instances of the *Callisto* application software are simultaneously run to control and collect data as determined by a scheduler configuration file. The scheduler file is setup to observe only during daylight hours and is updated

every other month. The FITS data files are transferred to the FHNW e-Callisto server in Switzerland. Data upload uses the File Transfer Protocol (FTP) driven by a *Perl* script. The Perl script is under control of the *System Scheduler* software application program that invokes the script at 15 minute intervals, corresponding to the FITS data intervals used by the Callistos. The PC uses the *Startup Delayer* software application to sequence and automatically load the Callisto software at PC startup.

Ancillary equipment includes a multi-voltage power supply system (5, 12, 15, 24 and 16 Vdc), uninterruptible power system (UPS) for the PC, web-controlled relay system and an industrial 4G cellular modem for internet access. The UPS is monitored by the *Power Panel* software application supplied with it. The *TeamViewer* software application is used to access the observatory from Anchorage. Cellular service is provided by AT&T 4G LTE service. A diversity antenna system at 18 m above ground level is used with the cellular modem to ensure adequate connection in the forested area where CRO is located. A *Web Power Switch* provides remote controlled relays for rebooting the Callistos and for controlling other power equipment in the observatory.



Author: Whitham Reeve is a contributing editor for the SARA journal, Radio Astronomy. He obtained B.S. and M.S. degrees in Electrical Engineering at University of Alaska Fairbanks, USA. He worked as a professional engineer and engineering firm owner/operator in the airline and telecommunications industries for more than 40 years and now manufactures electronic equipment used in radio astronomy. He has lived in Anchorage, Alaska his entire life. Email contact: whitreeve@gmail.com

Document information

Author: Whitham D. Reeve

Copyright: © 2018 W. Reeve

Revisions: 0.0 (Draft started 21 Nov 2017)
0.1 (Minor edits, 06 Jan 2018)
0.2 (Added noise storm characteristics and site data, 16 May 2018)
0.3 (Added observation plots, 28 May 2018)
0.4 (Minor edits, 09 Apr 2019)
0.5 (Updates before distribution, 25 May 2019)
0.6 (Distribution, 03 Jun 2019)

Word count: 3238

File size: 15523840